

THE EXTRAORDINARY FREQUENCY PATTERN VARIATION IN δ SCUTI STARS

L. A. BALONA

South African Astronomical Observatory, P.O. Box 9, Observatory 7935, Cape Town, South Africa
Version January 22, 2024

ABSTRACT

Inspection of the periodograms of *TESS* δ Scuti stars indicates that there is little, if any, similarity between the frequencies of stars in the same region of the H–R diagram. This is difficult to understand because pulsation models predict that stars with similar physical parameters should have similar frequencies. To investigate the problem, a quantitative measure of similarity between frequency patterns is described. When applied to non-adiabatic pulsation models with similar temperatures and luminosities, a strong correlation is found between the frequency patterns, as expected. The correlation remains high when rotational frequency splitting is included. When applied to observations, very little correlation can be found, confirming the impression from visual inspection. It seems that each star has its own unique frequency pattern, unrelated to its position in the H–R diagram. This presents a problem in our understanding of stellar pulsation. The existence of a period-luminosity law and the effect of combination frequencies in δ Scuti stars is briefly discussed.

Subject headings: stars:oscillations — stars:variables: δ Scuti

1. INTRODUCTION

Pulsational driving in models of A and F stars depends on the effective temperature, T_{eff} , luminosity, L/L_{\odot} , and chemical composition. Rotation has the effect of introducing additional frequencies. For stars located close together within a small region in the H–R diagram, the frequency spectra should be similar for stars with the same rotation rate. Differences in chemical composition will also affect the frequencies, but to a lesser extent. Furthermore, all stars within the instability strip should pulsate.

Inspection of the periodograms of several thousand δ Sct stars observed by *TESS* gives a strong impression that the above conclusions are not correct. Bedding et al. (2023) has recently remarked that the characteristics of the pulsation spectra in *TESS* δ Sct stars are varied and do not correlate with stellar temperature. More than half of the stars within the instability strip do not seem to pulsate at all (Balona 2018). The frequency patterns in γ Dor stars are very different from δ Sct stars, even though they might have the same effective temperature and luminosity. This cannot be attributed to rotation because the distribution of projected rotational velocities for γ Dor and δ Sct stars are the same.

Pulsation models cannot account for these observations. A better understanding of why certain pulsation modes are selected in preference to others is required. The study of mode selection in pulsating stars involves non-adiabatic, non-linear calculations for non-radial modes in rotating stars, which is beyond current capabilities. It is no surprise that scant attention has been paid to this problem. The review by Dziembowski

(1993) is still mostly relevant. For more recent work, see the excellent review by Smolec (2014).

The aim of this paper is to present a sample of periodograms to illustrate the problem. A method which measures the difference in frequency patterns in a quantitative way, while allowing for effects of rotation and chemical abundance, is described. This is applied to *TESS* δ Sct stars in several regions of the H–R diagram. The size of each region is sufficiently small that stars within it may be considered to have the same effective temperature and luminosity.

The calculations indicate that frequency patterns of stars within each region do not match at all. It is shown that rotation cannot account for the disparity. This means that there cannot be a general period - luminosity law for δ Sct stars (Poretti et al. 2008; McNamara 2011; Garg et al. 2010; Poleski et al. 2010; Cohen and Sarajedini 2012; Ziaali et al. 2019). The idea that combination frequencies may contribute to the disparity in frequency spectra can also be discarded.

2. DATA AND VARIABILITY CLASSIFICATION

Each *TESS* sector consists of about 27 d of continuous photometry with 2-min cadence. While stars near the ecliptic equator are only observed for one sector, stars near the ecliptic poles are observed in every sector. The light curves are corrected for instrumental signatures and long-term drift. These are called pre-search data conditioning (PDC) light curves. The data are from sectors 1–66 of the *TESS* mission.

As each sector becomes available, the light curves and periodograms of stars with $T_{\text{eff}} > 6000\text{K}$ are used to classify them according to variability type. The classification scheme follows that of the *General Catalogue of Variable Stars* (GCVS, Samus et al. 2017). In this way, many thousands of stars have been classified. A full de-

TABLE 1

DATA FOR ROTATING AND NON-ROTATING MODELS LOCATED WITHIN A SMALL REGION IN THE H–R DIAGRAM. THE FIRST COLUMN IS THE REGION NUMBER FOLLOWED BY THE CENTRAL $\log T_{\text{eff}}$ AND $\log L/L_{\odot}$ FOR THE REGION. THE LAST COLUMN IS THE NUMBER OF MODELS, N_{mod} , OR N_{obs} , THE NUMBER OF STARS, WITHIN EACH REGION.

Region	$\log T_{\text{eff}}$	$\log \frac{L}{L_{\odot}}$	N_{mod}	N_{obs}
(1,1)	3.85	0.695	13	129
(1,2)	3.85	0.945	5	747
(1,3)	3.85	1.195	10	468
(2,1)	3.87	0.821	7	726
(2,2)	3.87	1.071	4	1048
(2,3)	3.87	1.321	14	459
(3,1)	3.89	0.943	8	1099
(3,2)	3.89	1.193	5	748
(3,3)	3.89	1.443	14	356
(4,1)	3.91	1.063	6	899
(4,2)	3.91	1.313	5	468
(4,3)	3.91	1.563	15	206

scription of the identification and classification of *TESS* variables is given in Balona (2022b). As expected, most of the variables are of the δ Sct type. Among the 125000 stars already classified, there are 14000 δ Sct stars.

The *TESS* data present several problems in the classification of light variability. It seems that distinct regions of instability, as predicted by the models, do not actually exist. There is no region in the H–R diagram entirely free of pulsating stars (Balona and Ozuyar 2020). In order to assign a meaningful variability class, arbitrary boundaries in effective temperature, T_{eff} , and pulsation frequency, ν , must be defined. For example, the boundary between the δ Sct and Maia stars is set at $T_{\text{eff}} = 10000\text{K}$. The periodograms of these two classes of variable look the same: the Maia stars seem to be just an extension of the δ Sct instability strip to the early B stars (Balona 2023). The arbitrary boundaries in T_{eff} and ν are forced by the lack of a suitable theory, but are required to define the traditional classification scheme.

3. VARIETY OF FREQUENCY PATTERNS IN δ SCT STARS

To illustrate the variety of frequency patterns in δ Sct stars with similar stellar parameters, the instability strip was divided into 12 regions parallel to the zero-age main sequence (ZAMS), each region having a size $(\Delta \log T_{\text{eff}}, \Delta \log L/L_{\odot}) = (0.02, 0.25)$. This is sufficiently small that one may regard all stars within a region to have approximately the same effective temperature and luminosity, while at the same time sufficiently large to include a suitable number of stars. The region size also matches the uncertainties: $\sigma(\log T_{\text{eff}}) \approx 0.02$ and $\sigma(\log L/L_{\odot}) \approx 0.1$. Luminosities are from *GAIA DR3* parallaxes (Gaia Collaboration et al. 2016, 2021). Parameters of each region are listed in Table 1. Fig. 1 shows the names and locations of the regions in the H–R diagram.

Evolutionary stellar models were computed using the Warsaw - New Jersey evolution code (Paczynski 1970), assuming an initial hydrogen fraction, $X_0 = 0.70$ and metal abundance, $Z = 0.020$ and using the chemical element mixture of Asplund et al. (2009) and OPAL opac-

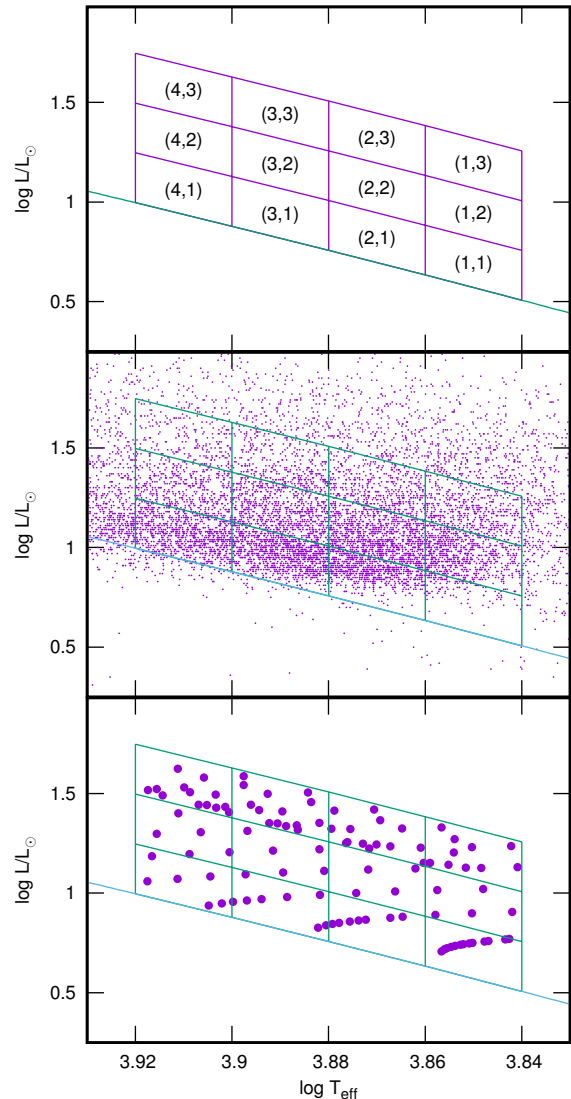


FIG. 1.— The top panel shows the location of the regions in the H–R diagram and the zero-age main sequence. The middle panel shows δ Sct stars detected by *TESS*, while the bottom panel shows models used in the analysis.

ities (Rogers and Iglesias 1992). Overshooting from the convective core was not included. A mixing length parameter $\alpha_{\text{MLT}} = 1.0$ was adopted for the convective scale height. All models are non-rotating. The non-adiabatic code developed by Dziembowski (1977b) was used to obtain the pulsation frequencies and growth rates. Pulsations in these models are purely driven by the opacity κ mechanism operating in the He II partial ionization region. The locations of the models in the H–R diagram are shown in the bottom panel of Fig. 1.

Examples of the disparity of frequency patterns within a given region are illustrated in Fig. 2. In each region, examples of three stars with rich frequency spectra and three stars with just a single dominant frequency peak are shown. In some cases one or two additional peaks are visible as well, but their amplitudes are always less than 5% of the amplitude of the main peak. About 5% of δ Sct stars have a single dominant peak defined in this way.

All stars have good spectroscopic estimates of T_{eff} . The

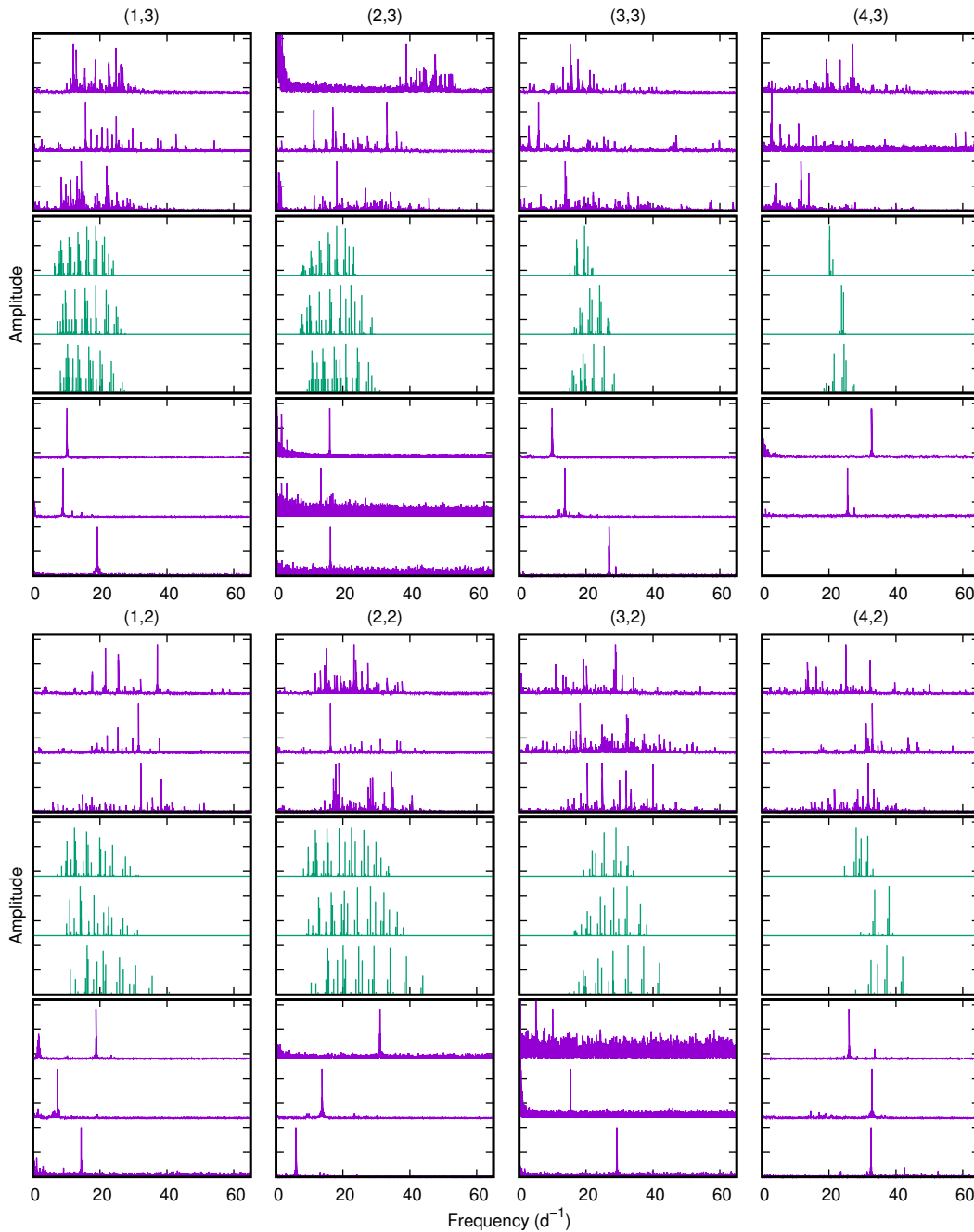


FIG. 2.— Illustration of the variety of frequency patterns in δ Sct stars compared with theoretical models. Each box consists of three panels. The top panel shows stars with rich frequency spectra, while stars with just a single dominant frequency peak are shown in the bottom panel. The middle panel (green) shows unstable frequencies from models. The label on the top of each box refers to a small region in the H–R diagram (Table 1).

middle row in Fig. 2 shows unstable modes from non-rotating models. The amplitudes were made to be proportional to the growth rate and corrected according to the visibility factor for the given spherical harmonic degree, l . Modes with $l \leq 8$ were selected.

The figure shows that stars with the same physical parameters can have completely different frequency patterns. Frequencies of single-mode stars may be very different from star to star within the same region. This indicates that the spherical harmonic degree and/or the radial order in these single-mode stars must differ from star to star. It is evident that the pattern in stars with rich

spectra cannot be obtained from rotational frequency splitting of the single-mode pulsators.

While Fig. 2 shows stars across the H–R diagram, Fig. 3 shows a larger sample of randomly chosen stars with similar, well determined, effective temperatures and luminosities in region (2,2). Each star seems to have its own unique frequency pattern.

4. CORRELATION

While a subjective impression of the disparity of frequency patterns can be obtained by inspection of Figs. 2 and 3, a method which quantitatively measures the de-

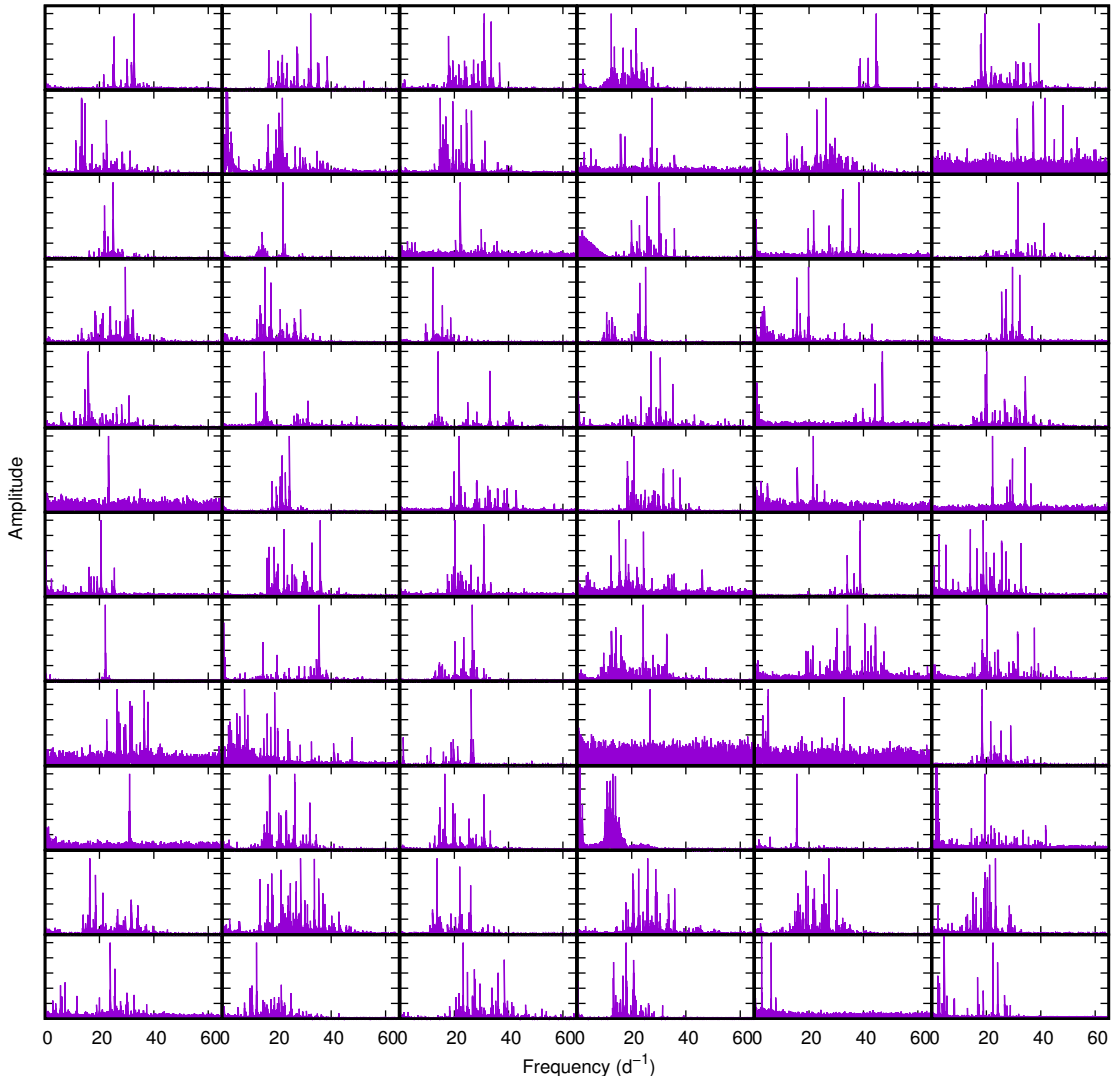


FIG. 3.— Examples of *TESS* δ Scuti periodograms for stars within a small region of the H–R diagram centered on $\log T_{\text{eff}} = 3.87$, $\log L/L_{\odot} = 1.07$ and with box size 0.02×0.025 dex.

gree of similarity between a pair of frequency patterns is required. One possibility is to calculate the correlation coefficient.

Suppose there are two frequency spectra, i and j , each sampled with equal frequency spacing, $\delta\nu$, between frequencies ν_1 and ν_2 . Let $y_i(\nu)$ and $y_j(\nu)$ be the amplitudes at frequency ν of spectra i and j . The correlation coefficient, r , between the two spectra is given by

$$r = \frac{1}{A_i A_j} \sum_{\nu=\nu_1}^{\nu_2} y_i(\nu) y_j(\nu) \delta\nu,$$

where A_i , A_j are constants. The values of these constants are chosen so that correlating a periodogram with itself gives unity. Thus

$$A_i^2 = \sum_{\nu=\nu_1}^{\nu_2} y_i^2(\nu) \delta\nu, \quad A_j^2 = \sum_{\nu=\nu_1}^{\nu_2} y_j^2(\nu) \delta\nu.$$

The value of r lies between $r = 0$ (no similarity) and $r = 1$ (periodograms are identical).

The appearance of a frequency pattern depends not

only on the frequencies, but also on the signal-to-noise ratio, S/N , and the amplitudes. Since all the observations discussed here were obtained by the same instrument, there should be no bias introduced by differing S/N ratios. The S/N ratio is mostly determined by the brightness of a star and, to a lesser extent, by the length of the time series. For stars within a given region, there will be approximately similar distributions of S/N and time series length, so these effects should average out.

In calculating the correlation coefficient, r , each extracted frequency peak can either be given the same weight or weighted according to its amplitude. In the models, the amplitude of a given mode is taken to be proportional to the growth rate. A visibility factor which depends on the spherical harmonic, l , is also applied. Trials on models with unit weight lead to a slightly broader distribution of r , as might be expected. The difference between weighting the frequency according to amplitude or assigning unit weight to all observed peaks in δ Sct stars is almost non-existent. This is owing to the fact that r is always close to zero, as demonstrated below. In the results derived here, the frequency distributions are

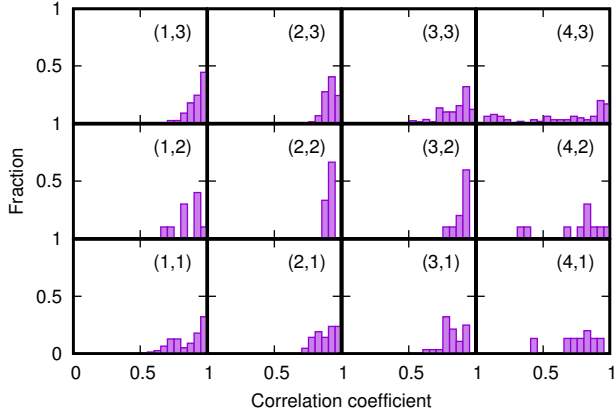


FIG. 4.— Distribution of correlation coefficients for non-rotating models in each region.

always weighted according to amplitude (with visibility factor applied for models), as this seems more realistic.

Given any two stars, the extracted pulsation frequencies will never be exactly the same. This means that the value of r will always be near zero if the frequency bin is very small. This problem is avoided by constructing a histogram of the frequency distribution with a suitable frequency bin size, $\delta\nu$. In selecting a suitable bin size, it is important to examine the range of frequencies that might be expected for stars within the same region in the H–R diagram.

Examination of pulsation models within a range of 0.02 dex in $\log T_{\text{eff}}$ and 0.25 dex in $\log L/L_{\odot}$ shows that for a fixed spherical harmonic degree and radial order (l, n), the rms scatter in the frequencies is typically 2–6 d^{-1} . This can be higher for g modes or mixed modes. A change in abundance leads to a somewhat different convective core size. Since g modes mostly sample the interior of a star near the convective core, there can be changes in frequencies of some g modes, but these are only of the order of several microhertz (Guzik et al. 1998). This is smaller than the effect of rotation. Other effects, such as mass loss and the presence of a magnetic field, do not alter the mean density and, in most cases, have very little effect on the pulsation frequencies.

Choosing a bin size $\delta\nu = 4, 5$ or 6 d^{-1} results in only slight differences in the resulting distribution of correlation coefficients for the models and almost no difference at all for the observations. Below $\delta\nu = 3 \text{ d}^{-1}$ the distributions begin to show an increasing noise level which tends to obscure any correlation that may be present. This is to be expected as a smaller bin size leads to less overlap between distributions. If the value of $\delta\nu$ is too large, the overlap between frequency distributions will increase and the distribution of r will flatten and start to lose its discriminatory power. This begins to occur when $\delta\nu = 7 \text{ d}^{-1}$ in the models. A value of $\delta\nu = 5 \text{ d}^{-1}$ was chosen as being a good compromise.

5. CORRELATION FROM PULSATION MODELS

A small change in effective temperature and luminosity in a model of a non-rotating star will lead to small changes in the predicted frequencies. It is therefore expected that the frequency distributions derived from models with similar values of ($\log T_{\text{eff}}, \log L/L_{\odot}$) will be strongly correlated. The aim of this section is to show

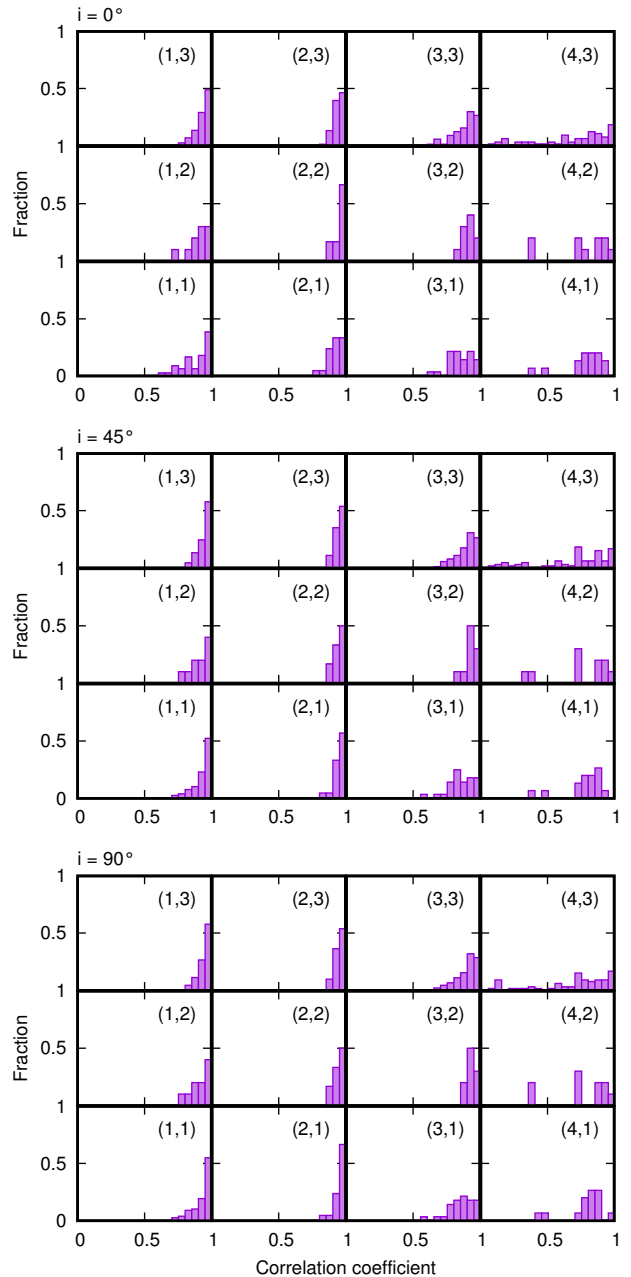


FIG. 5.— Distribution of correlation coefficients when rotational splitting is applied. The inclination of the axis of rotation is fixed for all stars. The inclinations are $i = 0^\circ$ (top panel) $i = 45^\circ$ (middle panel) and $i = 90^\circ$ (bottom panel).

that this is indeed the case. It is also important to study how the correlation coefficient might change between models with different rotation rates. When calculating the correlation coefficient between model spectra, the amplitudes are taken to be proportional to the growth rate. In addition, a visibility factor which depends on the spherical harmonic degree, l , is applied.

For a model in a particular region, the correlation coefficient between the frequency pattern of unstable modes was correlated with the frequency pattern for all other models in the region. The number of models for each region, N_{mod} , is shown in Table 1. Each pair of models gives rise to one correlation coefficient, r . The resulting distribution of r for all pairs of non-rotating models is

shown in Fig. 4. As expected, the distribution of r tends to concentrate near $r = 1$.

Reese et al. (2006) provides a formula for third-order rotational perturbation as well as the necessary coefficients for $l \leq 3$. For higher values of l , coefficients for $l = 3$ were used. The distribution of rotational equatorial velocities for mid-A stars (Balona 2022a) was used to derive the distribution of rotational frequencies required in the formula.

To test the effect of rotation, frequency splitting was applied to each unstable mode with spherical harmonic degree l , so that a frequency in the non-rotating model is replaced by $2l + 1$ frequencies. The relative amplitudes of the multiplets vary according to $P_l^{lm}(\cos i)$ (Eq. 6 of Dziembowski 1977a or Eq. 17 of Gizon and Solanki 2003). The resulting distributions are shown in Fig. 5 for three fixed inclination angles of $i = 0^\circ$, $i = 45^\circ$ and $i = 90^\circ$. Once again, the values of r tend to be close to unity.

The models indicate that one should expect a high level of correlation of frequency patterns for δ Sct stars within a given region. Furthermore, it suggests that differing rotation rates among the stars do not affect the correlation very much at all.

6. CORRELATION FROM OBSERVATIONS

As can be seen from Fig. 1 and Table 1, each region is well populated with δ Sct stars. On average, there are about 600 stars in each of the 12 regions. It is important that a sufficiently large number of stars is used because the errors in $\log T_{\text{eff}}$ and $\log L/L_\odot$ are comparable to the region size. Systematic errors are also present. For example, rapid rotation tends to shift the apparent effective temperature due to gravity darkening. The mean equatorial velocities for A/F stars is around $v_e \approx 80 \text{ km s}^{-1}$ (Balona 2022a), whereas the typical critical rotational velocity is $v_c \approx 400 \text{ km s}^{-1}$ ($v_e/v_c \approx 0.2$). Significant systematic effects due to gravitational darkening only begin for $v_e/v_c \gtrsim 0.5$ (see Fig. 4 in Salmon et al. 2014), so this effect is likely to be small.

The visibility of a pulsation peak also depends on the angle of inclination, i . A variation in i leads only to a variation in amplitude, not frequency, but will still tend to lower the correlation. Since i is randomly distributed, most stars will be observed close to $i \approx 90^\circ$ because the number of stars observed with inclination i is distributed as $\sin i$. For this reason, the effect of differing angles of inclination is likely to be small as well.

Frequencies of δ Sct stars were extracted from the periodograms. The extracted frequency is deemed significant if the signal-to-noise ratio in the amplitude exceeds 4.7. Each significant extracted frequency peak was assigned a weight proportional to its amplitude when calculating the histogram of the frequency distribution. As before, the correlation coefficients, r , were obtained for all possible pairs of stars within a given region. Finally, the distribution of r for each region was determined.

The calculation was performed for 1673 stars with precise measurements of effective temperature as well as 7353 stars for which any estimate of effective temperature was accepted. The results are very similar. In Table 1, N_{obs} is the number of stars in each region for the latter case. The distributions of correlation coefficients

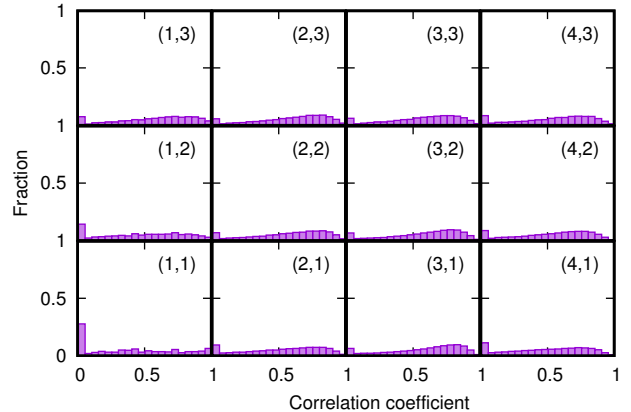


FIG. 6.— Distribution of correlation coefficients for *TESS* δ Sct stars within a small region in the H–R diagram.

are shown in Fig. 6.

Fig. 6 shows that, contrary to the model predictions, there is very little correlation between the frequency patterns in δ Sct stars with similar effective temperatures and luminosities. As discussed above, rotation does not affect the correlation coefficient very much at all. Therefore, one can rule out rotation as the cause of the observed small correlations.

7. MODE COUPLING

Mode coupling involving non-linear mode interactions between two or more modes may result in a complex frequency spectrum which could account for the wide disparity in the frequency patterns in δ Sct stars. Mourabit and Weinberg (2023) used the theory of three-mode coupling to study the strength and prevalence of non-linear mode interactions in δ Sct models across the instability strip. They conclude that resonant mode interactions can be significant. Mode coupling may explain the rapid changes in amplitude and frequency seen in some δ Sct stars (Bowman et al. 2016, 2021).

A combination frequency involving two parent modes, ν_1, ν_2 is given by $\nu = n_1\nu_1 + n_2\nu_2$ where n_1, n_2 are positive or negative integers. If the frequency ν matches an observed frequency peak to within the observational error, then ν can be regarded as a combination frequency. To test the degree of mode coupling that may be present in δ Sct stars, all possible combination frequencies with $|n_1| \leq 7$ and $|n_2| \leq 7$ were identified among 6840 δ Sct stars with at least five significant peaks.

It was found that at least one or more combination frequencies are present in 4151 stars (60 percent of the total), but in most of these stars only a small fraction of the frequency peaks are identified as combination frequencies. The distribution of stars with combination frequencies is shown in Fig. 7.

Higher order combinations involving three or even more modes could occur, but these would be difficult to identify. Considering that very few combination frequency peaks were identified in most stars, it is very unlikely that mode interaction may be the explanation for the diversity of frequency patterns.

8. PERIOD–LUMINOSITY RELATION

Considering the large disparity in frequency patterns at constant temperature and luminosity, it would be sur-

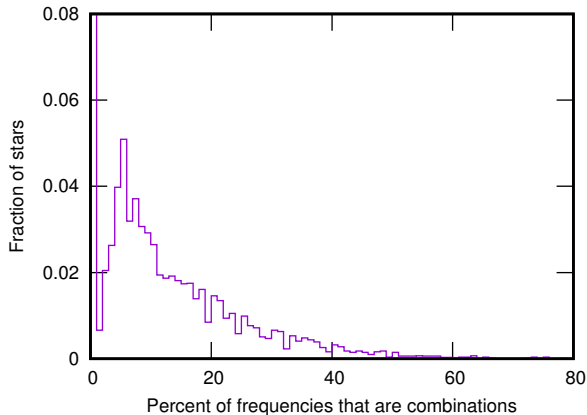


FIG. 7.— Fraction of δ Sct stars as a function of percentage of frequencies that are combinations.

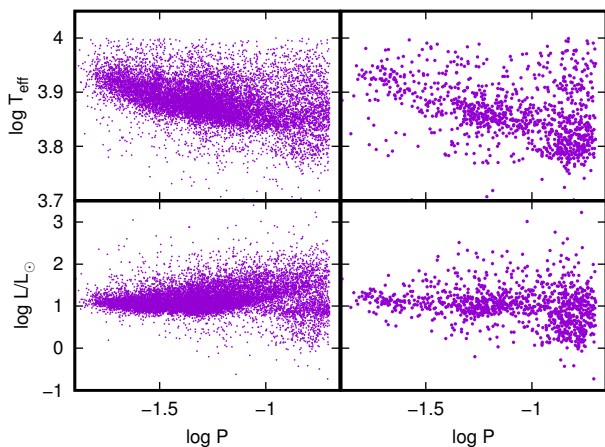


FIG. 8.— Effective temperature and luminosity as a function of pulsation period, P (days), using the period which corresponds to the peak with highest amplitude in *TESS* δ Sct stars. The left panels include all stars, while the panels on the right are restricted to stars with one dominant frequency.

prising if a period–luminosity law, similar to the Cepheid P–L law, can be found for δ Sct stars. Nevertheless, the existence of a P–L relation in δ Sct stars has been reported from time to time. Since there are usually many periods to be chosen in any given δ Sct star, the period corresponding to the highest amplitude is used. Barac et al. (2022) found that stars lie on a ridge that corresponds to pulsation in the fundamental radial mode, while others pulsate in shorter period overtones. The correlation is best seen in the period - mean density relationship.

It should be borne in mind that there are several correlations between the pulsation period, P , and the physical parameters. Pulsations in δ Sct stars are mainly driven by the κ opacity mechanism operating in the He II partial ionization zone. In cool stars, the zone is deep, the resonant cavity is large and the radial order of the pulsations is low, so the periods are typically long. In hot stars, the zone is shallow, the resonant cavity is small and the radial order is high, so the periods are shorter. This effect can be seen in the model frequencies in Fig. 2.

From the observations of 11833 δ Sct stars, the frequency of maximum amplitude was extracted. The left panels of Fig. 8 shows the relationship between $\log T_{\text{eff}}$

and $\log P$ (top panel) and between $\log L/L_{\odot}$ and $\log P$ (bottom panel). As predicted by the models, the pulsation period decreases as the temperature increases, though the correlation is not particularly strong. However, there is no significant correlation between $\log P$ and $\log L/L_{\odot}$.

It is possible that stars with a single dominant mode may be best suited to test the idea of a P–L relationship because these could be radial modes (or at least non-radial modes of the same degree). The corresponding relationships for these stars are shown in the right panels of Fig. 8. Once again, the only correlation is between $\log T_{\text{eff}}$ and $\log P$. This indicates that modes in stars with only one dominant frequency do not have the same value of l or radial order.

In conclusion, there seems to be a weak correlation between the dominant pulsation period and effective temperature in δ Sct stars, in agreement with model predictions. García Hernández et al. (2015) analyzed δ Sct stars in eclipsing binaries and derived an observational scaling relation between the stellar mean density and a frequency pattern in the oscillation spectrum which is independent of rotation rate. It is possible that careful analyses of selected stars with well-determined physical parameters in this manner might lead to reliable mode identification in some δ Sct stars. However, a universal period – luminosity law similar to that in Cepheids does not seem to exist.

9. DISCUSSION AND CONCLUSIONS

The surprisingly wide variety of frequency patterns in δ Sct stars has been noted several times (e.g. Balona et al. 2015; Bedding et al. 2023). Inspection of many thousands of periodograms gives the impression that each δ Sct star has a unique set of frequencies, unrelated to its location in the H–R diagram.

In this paper, periodograms of δ Sct stars observed by *TESS* are presented. These are shown for stars that lie within small regions of the H–R diagram. In each region, where stars have essentially the same effective temperature and luminosity, stars can be found with just a single frequency peak and also with many frequency peaks. This is in contradiction to pulsation models which predict that stars with the same global parameters and rotation rates should pulsate with the same set of frequencies.

In order to obtain an objective measure of similarity of frequency patterns in a pair of stars, a correlation method was developed. Using non-adiabatic non-rotating pulsation models, it is found that the frequencies of unstable modes within a small effective temperature and luminosity range are indeed correlated. The effect of rotation was simulated by applying rotational splitting using a 3rd-order approximation formula (Reese et al. 2006). A spread of rotation periods similar to that expected for mid-A stars was used. The results show that the correlations among rotating stars are as high as among non-rotating stars.

When applied to a large sample of *TESS* δ Sct stars with similar effective temperatures and luminosities, very little correlation is found. In other words, the observed frequencies are not related to the location of the star in the H–R diagram at all. This is in contradiction to what is found in the models.

The possibility that combination frequencies may be

responsible for some of the discrepancy seems unlikely. Although combination frequencies were detected in about 60 percent of the stars, they constitute only a small fraction of the total number of frequency peaks observed in a star.

The fact that frequencies in δ Sct stars with similar effective temperatures and luminosities vary so widely indicates that there is no possibility of finding a useful period - luminosity relation. Even for stars where only one dominant mode is present, the frequency of this mode can vary widely between stars with essentially the same physical parameters. This means that the spherical harmonic degree and/or radial order must differ from star to star. However, there is a general trend for the hotter, more luminous stars to have shorter pulsation periods, in agreement with non-adiabatic pulsation models.

The effect described here suggests that there is a fundamental problem with current models. It is clear that the excitation of modes is a highly non-linear process which perhaps involves mode interaction. Current models also do not accurately describe the outer layers of A and F stars. The likely presence of starspots and even flares on early-type stars (Balona 2021) indicates a complex structure. It is possible that local conditions may determine the frequencies that are selected.

Progress might be achieved by including the effect of surface convection, even in the hottest models of δ Sct stars. An attempt should be made on modifying the pulsational parameters in these models to determine if a wide variety of unstable frequencies can thereby be obtained. The possible effect of photospheric structures on the number of observed pulsation peaks could be studied using high-dispersion spectroscopy. Observations of stars with a single dominant mode and stars with very rich frequency spectra may provide clues to the difference in mode selection and the extreme sensitivity of pulsational driving to local conditions.

ACKNOWLEDGMENTS

I thank the National Research Foundation of South Africa for financial support and Dr. W. Dziembowski for permission to use his code.

This paper includes data collected by the *TESS* mission. Funding for the *TESS* mission is provided by the NASA Explorer Program. Funding for the *TESS* Asteroseismic Science Operations Centre is provided by the Danish National Research Foundation (Grant agreement no.: DNR106), ESA PRODEX (PEA 4000119301) and Stellar Astrophysics Centre (SAC) at Aarhus University. We thank the *TESS* and TASC/TASOC teams for their support of the present work.

This work has made use of data from the European Space Agency (ESA) mission Gaia (<https://www.cosmos.esa.int/gaia>), processed by the Gaia Data Processing and Analysis Consortium (DPAC), <https://www.cosmos.esa.int/web/gaia/dpac/consortium>). Funding for the DPAC has been provided by national institutions, in particular the institutions participating in the Gaia Multilateral Agreement.

This research has made use of the SIMBAD database, operated at CDS, Strasbourg, France. This research has made use of the VizieR catalogue access tool, CDS, Strasbourg, France (DOI: 10.26093/cds/vizieR). The original description of the VizieR service was published in *A&AS* 143, 23.

The data presented in this paper were obtained from the Mikulski Archive for Space Telescopes (MAST). STScI is operated by the Association of Universities for Research in Astronomy, Inc., under NASA contract NAS5-2655.

DATA AVAILABILITY

The data underlying this article can be obtained from <https://sites.google.com/view/tessvariables/home>.

REFERENCES

- M. Asplund, N. Grevesse, A. J. Sauval, and P. Scott. The Chemical Composition of the Sun. *ARA&A*, 47:481–522, September 2009. doi:10.1146/annurev.astro.46.060407.145222.
- L. A. Balona. Gaia luminosities of pulsating A-F stars in the Kepler field. *MNRAS*, 479:183–191, September 2018. doi:10.1093/mnras/sty1511.
- L. A. Balona. Spots and Flares in Hot Main Sequence Stars Observed by Kepler, K2, and TESS. *Frontiers in Astronomy and Space Sciences*, 8:32, 2021. doi:10.3389/fspas.2021.580907. URL <https://www.frontiersin.org/article/10.3389/fspas.2021.580907>
- L. A. Balona. Rotation of hot normal, peculiar and Be stars from space photometry. *MNRAS*, 516(3):3641–3649, November 2022a. doi:10.1093/mnras/stac2515.
- L. A. Balona. Maia variables and other anomalies among pulsating stars. *Frontiers in Astronomy and Space Sciences*, 10:1266750, September 2023. doi:10.3389/fspas.2023.1266750.
- L. A. Balona and D. Ozuyar. Pulsation among TESS A and B stars and the Maia variables. *MNRAS*, 493(4):5871–5879, March 2020. doi:10.1093/mnras/staa670.
- L. A. Balona, J. Daszyńska-Daszkiewicz, and A. A. Pamyatnykh. Pulsation frequency distribution in δ Scuti stars. *MNRAS*, 452:3073–3084, September 2015. doi:10.1093/mnras/stv1513.
- Luis A. Balona. Identification and classification of TESS variable stars. *arXiv e-prints*, art. arXiv:2212.10776, December 2022b.
- Natascha Barac, Timothy R. Bedding, Simon J. Murphy, and Daniel R. Hey. Revisiting bright δ Scuti stars and their period-luminosity relation with TESS and Gaia DR3. *MNRAS*, 516(2):2080–2094, October 2022. doi:10.1093/mnras/stac2132.
- Timothy R. Bedding, Simon J. Murphy, Courtney Crawford, Daniel R. Hey, Daniel Huber, Hans Kjeldsen, Yaguang Li, Andrew W. Mann, Guillermo Torres, Timothy R. White, and George Zhou. TESS Observations of the Pleiades Cluster: A Nursery for δ Scuti Stars. *ApJ*, 946(1):L10, March 2023. doi:10.3847/2041-8213/acc17a.
- D. M. Bowman, D. W. Kurtz, M. Breger, S. J. Murphy, and D. L. Holdsworth. Amplitude modulation in δ Sct stars: statistics from an ensemble study of Kepler targets. *MNRAS*, 460:1970–1989, August 2016. doi:10.1093/mnras/stw1153.
- D. M. Bowman, J. Hermans, J. Daszyńska-Daszkiewicz, D. L. Holdsworth, A. Tkachenko, S. J. Murphy, B. Smalley, and D. W. Kurtz. KIC 5950759: a high-amplitude δ Sct star with amplitude and frequency modulation near the terminal age main sequence. *MNRAS*, 504(3):4039–4053, July 2021. doi:10.1093/mnras/stab1124.
- Roger E. Cohen and Ata Sarajedini. SX Phoenixis period-luminosity relations and the blue straggler connection. *MNRAS*, 419(1):342–357, January 2012. doi:10.1111/j.1365-2966.2011.19697.x.
- W. Dziembowski. Light and radial velocity variations in a nonradially oscillating star. *Acta Astronomica*, 27:203–211, 1977a.
- W. Dziembowski. Oscillations of giants and supergiants. *Acta Astron.*, 27:95–126, 1977b.

- W. A. Dziembowski. Mode selection and other nonlinear phenomena in stellar oscillations. In W. W. Weiss and A. Baglin, editors, *IAU Colloq. 137: Inside the Stars*, volume 40 of *Astronomical Society of the Pacific Conference Series*, pages 521–534, January 1993.
- Gaia Collaboration, T. Prusti, J. H. J. de Bruijne, A. G. A. Brown, A. Vallenari, C. Babusiaux, C. A. L. Bailer-Jones, U. Bastian, M. Biermann, D. W. Evans, and et al. The Gaia mission. *A&A*, 595:A1, November 2016. doi:10.1051/0004-6361/201629272.
- Gaia Collaboration, A. G. A. Brown, A. Vallenari, T. Prusti, J. H. J. de Bruijne, C. Babusiaux, M. Biermann, O. L. Creevey, D. W. Evans, and et al. Gaia Early Data Release 3. Summary of the contents and survey properties. *A&A*, 649:A1, May 2021. doi:10.1051/0004-6361/202039657.
- A. García Hernández, S. Martín-Ruiz, M. J. P. F. G. Monteiro, J. C. Suárez, D. R. Reese, J. Pascual-Granado, and R. Garrido. Observational Delta nu - rho Relation for δ Sct Stars using Eclipsing Binaries and Space Photometry. *ApJ*, 811:L29, October 2015. doi:10.1088/2041-8205/811/2/L29.
- A. Garg, K. H. Cook, S. Nikolaev, M. E. Huber, A. Rest, A. C. Becker, P. Challis, A. Clochiatti, G. Miknaitis, D. Minniti, L. Morelli, K. Olsen, J. L. Prieto, N. B. Suntzeff, D. L. Welch, and W. M. Wood-Vasey. High-amplitude δ -Scutis in the Large Magellanic Cloud. *AJ*, 140(2):328–338, August 2010. doi:10.1088/0004-6256/140/2/328.
- L. Gizon and S. K. Solanki. Determining the Inclination of the Rotation Axis of a Sun-like Star. *ApJ*, 589(2):1009–1019, June 2003. doi:10.1086/374715.
- J. A. Guzik, M. R. Templeton, and P. A. Bradley. The Effects of Metallicity on Delta Scuti Star Asteroseismology. In Paul A. Bradley and Joyce A. Guzik, editors, *A Half Century of Stellar Pulsation Interpretation*, volume 135 of *Astronomical Society of the Pacific Conference Series*, page 470, January 1998.
- D. H. McNamara. Delta Scuti, SX Phoenicis, and RR Lyrae Stars in Galaxies and Globular Clusters. *AJ*, 142(4):110, October 2011. doi:10.1088/0004-6256/142/4/110.
- Mohammed Mourabit and Nevin N. Weinberg. Resonant Mode Coupling in δ Scuti Stars. *ApJ*, 950(1):6, June 2023. doi:10.3847/1538-4357/acca16.
- B. Paczyński. Evolution of Single Stars. I. Stellar Evolution from Main Sequence to White Dwarf or Carbon Ignition. *Acta Astron.*, 20:47, 1970.
- R. Poleski, I. Soszyński, A. Udalski, M. K. Szymański, M. Kubiak, G. Pietrzyński, L. Wyrzykowski, O. Szweczyk, and K. Ulaczyk. The Optical Gravitational Lensing Experiment. The OGLE-III Catalog of Variable Stars. VI. Delta Scuti Stars in the Large Magellanic Cloud. *Acta Astron.*, 60(1):1–16, March 2010. doi:10.48550/arXiv.1004.0950.
- Ennio Poretti, Gisella Clementini, Enrico V. Held, Claudia Greco, Mario Mateo, Luca Dell’Arciprete, Luca Rizzi, Marco Gullieuszik, and Marcella Maio. Variable Stars in the Fornax dSph Galaxy. II. Pulsating Stars below the Horizontal Branch. *ApJ*, 685(2):947–957, October 2008. doi:10.1086/591241.
- D. Reese, F. Lignières, and M. Rieutord. Acoustic oscillations of rapidly rotating polytropic stars. II. Effects of the Coriolis and centrifugal accelerations. *A&A*, 455:621–637, August 2006. doi:10.1051/0004-6361:20065269.
- F. J. Rogers and C. A. Iglesias. Radiative atomic Rosseland mean opacity tables. *ApJS*, 79:507–568, April 1992. doi:10.1086/191659.
- S. J. A. J. Salmon, J. Montalbán, D. R. Reese, M.-A. Dupret, and P. Eggenberger. The puzzling new class of variable stars in NGC 3766: old friend pulsators? *A&A*, 569:A18, September 2014. doi:10.1051/0004-6361/201323259.
- N. N. Samus, E. V. Kazarovets, O. V. Durlevich, N. N. Kireeva, and E. N. Pastukhova. General catalogue of variable stars: Version GCVS 5.1. *Astronomy Reports*, 61(1):80–88, Jan 2017. doi:10.1134/S1063772917010085.
- R. Smolec. Mode selection in pulsating stars. In J. A. Guzik, W. J. Chaplin, G. Handler, and A. Pigulski, editors, *Precision Asteroseismology*, volume 301 of *IAU Symposium*, pages 265–272, February 2014. doi:10.1017/S1743921313014439.
- Elham Ziaali, Timothy R. Bedding, Simon J. Murphy, Timothy Van Reeth, and Daniel R. Hey. The period-luminosity relation for δ Scuti stars using Gaia DR2 parallaxes. *MNRAS*, 486(3):4348–4353, July 2019. doi:10.1093/mnras/stz1110.

provides fast and easy peer review for new papers in the **astro-ph** section of the arXiv, making the reviewing process simpler for authors and referees alike. Learn more at <http://astro.theoj.org>.

This paper was built using the Open Journal of Astrophysics L^AT_EX template. The OJA is a journal which